Effect of reinforcing submicron SiC particles on the wear of electrolytic NiP coatings Part 1. Uni-directional sliding

I.R. Aslanyan, J.-P. Bonino and J.-P. Celis

Katholieke Universiteit Leuven, Departement Metaalkunde en Toegepaste Materiaalkunde, Kasteelpark Arenberg 44, B-3001 Leuven, Belgium

Russian Academy of Sciences, Institute for Metals Superplasticity Problems, Khalturina 39, Ufa 450001, Russia

Université Pierre Sabatier, Toulouse, France

Abstract

As-plated and annealed NiP coatings and composite NiP–SiC coatings were investigated in uni-directional ball-on-disc sliding tests. Abrasive wear was noticed in the case of composite NiP coatings containing submicron SiC particles, whereas in NiP coatings oxidational wear was active. The addition of submicron SiC particles not only increases the hardness of these electrolytic coatings but also hinders the formation of an oxide film in the sliding wear track. As a consequence, the wear loss on as-plated NiP coatings is not markedly reduced by the addition of SiC particles. On the contrary, a heat treatment at 420 °C for 1 h decreases the wear loss on both pure NiP and composite NiP–SiC coatings. During that heat treatment, Ni_3P precipitates are formed in the NiP matrix and owing to this fact, the hardness of both pure NiP and composite NiP–SiC coatings increases. However, the heat treatment of composite NiP–SiC coatings induces the sensitivity for crack formation in the NiP matrix around these SiC particles. As a result, the pull out of SiC particles in the wear track occurs easily during sliding, and the wear loss of composite NiP–SiC coatings remains above the wear loss on NiP coatings.

Keywords: Composite coatings; Friction; Wear; Oxides; Heat treatment

1. Introduction

2. Experimental

3. Results and discussion

4. Conclusions

Acknowledgements

References

1. Introduction

The interest for electroplated composite nickel was initiated by the promising friction and wear results obtained with other nanocrystalline materials [1] and [2], and the ability to produce coatings with a very small grain size by electrodeposition [3] and [4]. Previous investigations [5], [6] and [7] on Ni-based coatings revealed a significant improvement of the wear resistance resulting from the incorporation of SiC particles in the nickel matrix. Moreover, the wear resistance increases with the addition of phosphorus to the nickel matrix [8]. The combination of Ni_3P precipitates and embedded SiC particles was reported as a most cost-effective and best-performing combination in applications where abrasive wear resistance is the main requirement [9] and [10].

Early investigations on composite NiP and NiP–SiC with mean size of SiC particles values about 45 µm coatings revealed the occurrence of abrasive wear in NiP composite coatings after a limited number of 400 cycles [8]. However, at 400 cycles, the running-in phase is still on-going, and the wear behavior may evolve during further testing. According to Huang et al. [11], the wear rate of NiP and NiP–SiC coatings with an average size of SiC particles of about 4.5 µm is comparable. Details on wear test conditions were unfortunately not reported. Taheri et al. [12] studied the tribological behavior of electroless NiP coatings but did not report on neither the wear rate of these coatings nor on possible wear mechanisms. Berkh et al. [13] investigated the wear behavior of electrodeposited NiP–SiC composite coatings containing 6–7 wt.% P. Dry wheel abrasion tests were performed for a sliding distance of 42.5 m. However, at that short sliding distance, the running-in stage is most probably still in progress. They reported that the wear rate decreases with increasing SiC particles content with mean size values between 3.28 and 1.14 µm for both as-plated and heat-treated coatings.

The aim of this work is to understand the effect of incorporated submicron SiC particles in electrolytic NiP coatings on the friction and wear evolution during uni-directional sliding tests. The wear mechanisms active under such contact conditions on pure and composite electrolytic Ni–P coatings are discussed.

2. Experimental

NiP coatings were deposited on steel substrates from an electrolytic plating bath containing a suspension of 0, 80 or 200 g/l SiC particles with a mean diameter of 600 nm. The plating solution contained 20 g/l H_3PO_3. Part of the samples was heat-treated at 420 °C for 1 h in atmosphere.

Metallographic cross-sections of the samples were prepared by grinding and polishing without using any SiC abrasive paper in order to avoid any contamination of the composite coatings by

foreign SiC particles. Vickers microhardness measurements were carried out at a load of 50 g, and nanoindentation was done in the wear track areas.

X-ray diffraction spectra were recorded by a Seifert 3003TT-powder diffractometer using CuKα radiation at an incidence angle of 2°. The changes in structure induced by heat treatment were detected in that way.

Uni-directional sliding ball-on-disc wear tests were performed at normal loads of 2 and 5 N, and a constant sliding speed of 0.15 m/s. The wear track diameter was 24 mm and the rotation speed of the disc was 60 rpm. The contact frequency was thus 1 Hz. The number of rotations was set at either 100, 1000 or 15,000. All the wear tests were performed against 10 mm diameter corundum balls (Ceratech, The Netherlands) with a surface roughness of approximately 0.2 μm (Ra), without lubrication, at 23 °C, and in ambient air of 50% relative humidity. The tangential friction force was recorded continuously during the sliding wear tests.

The surface morphology of coatings and wear tracks were examined by scanning electron microscopy (SEM-Philips 515). Chemical analyses were done by EDAX at acceleration voltages of 10 and 20 kV. Some worn samples were investigated before and after ultrasonic cleaning for 15 min in ethanol.

The volumetric material loss after the wear tests, and the surface roughness were determined by white light interferometer (Wyko NT Series, Optical 3D Profiling Systems). Some samples were cleaned in ethanol under ultrasonic agitation for 15 min.

3. Results and discussion

The morphology of the NiP coatings is shown in Fig. 1a. These coatings have a nodular surface structure, a low roughness, Ra, of about 13 nm, and in a visual inspection they have a light gray color with a luster effect. The heat treatment at 420 °C for 1 h does not affect to a measurable extent neither the roughness nor the microstructure.

Fig. 1. SEM micrographs of as-plated composite NiP–SiC coatings: (a) electrolytic NiP, (b) electrolytic NiP–SiC from bath with 80 g/l of 600 nm SiC particles; and (c) electrolytic NiP–SiC from bath with 200 g/l of 600 nm SiC particles.
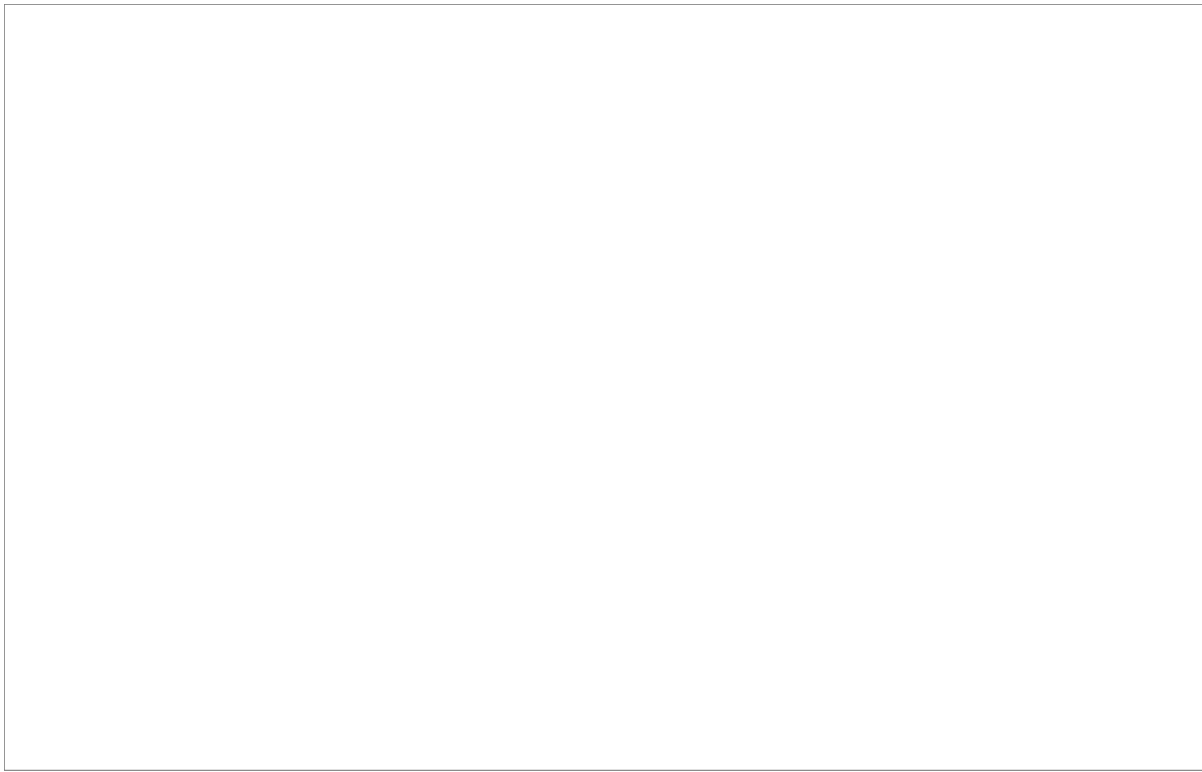
The morphology of the NiP–SiC coatings consists of a homogeneous fine globular structure with embedded SiC particles appearing as white spots. Fig. 1b and c show the representative morphology of as-plated coatings produced from baths containing 80 and 200 g/l SiC particles, respectively. The chemical composition of these NiP–SiC coatings is quite similar (Table 1), as well as their morphology. The morphology and microstructure of these coatings is not modified by the heat treatment at 420 °C for 1 h. The roughness, Ra, is about 50 nm for both as-plated and heat-treated composite NiP–SiC coatings. As generally experienced, composite coatings are rougher than the particle-free deposits due to the entrapment of particles. During electrolytic codeposition, the metal matrix may grow on top of the slightly conductive SiC-particles, and at the end of the electrodeposition some parts of the SiC-particles may stick out of the metal matrix. From Fig. 2, it is evident that the 600 nm diameter SiC particles are embedded as individual particles in the as-plated NiP matrix. They are rather homogeneously distributed in that matrix both in the outermost layer of the coatings (Fig. 2) as through the coating thickness (see Fig. 3). In such cross-sectional views, cracks were not noticed in as-plated composite NiP–SiC coatings. On the contrary, cracks

were sometimes observed at the interface between coatings and substrate. The thickness of all the coatings investigated was in the range of 20 to 30 μm.

Table 1.

EDX compositional analyses of wear tracks on as-plated and heat-treated pure NiP and composite NiP–SiC coatings, and on some debris formed during uni-directional sliding tests

| Coatings investigated		Number of sliding contacts	EDX analyses after uni-directional sliding tests at 2 N and 0.1 m/s in ambient air of 50% RH and 23 °C					
			Elements, wt.%					
			Ni	P	Si	C	O	Al
NiP–SiC (bath 80 g/l SiC)	As-plated	15,000	64.63	10.79	4.78	2.51	16.59	1.33
	Heat-treated		74.59	9.92	5.18	7.67	2.64	0.70
	Debris		46.28	5.76	6.01	12.43	28.20	1.33
NiP–SiC (bath 200 g/l SiC)	As-plated	15,000	62.56	10.51	5.91	3.08	17.94	1.09
	Heat-treated		77.81	10.61	5.58	6.00	—	—
	Debris		31.75	4.42	12.00	15.83	34.08	1.93
NiP	As-plated	100	86.89	13.11	—	—	—	—
		1000	83.12	12.81	—	—	4.07	—
		15,000	72.04	9.61	—	—	17.05	1.30
	Heat-treated	100	87.21	12.79	—	—	—	—
		1000	82.17	11.76	—	—	6.07	—
		15,000	68.17	9.57	—	—	21.14	1.13
	Debris	15,000	62.78	8.03	—	—	26.85	2.33
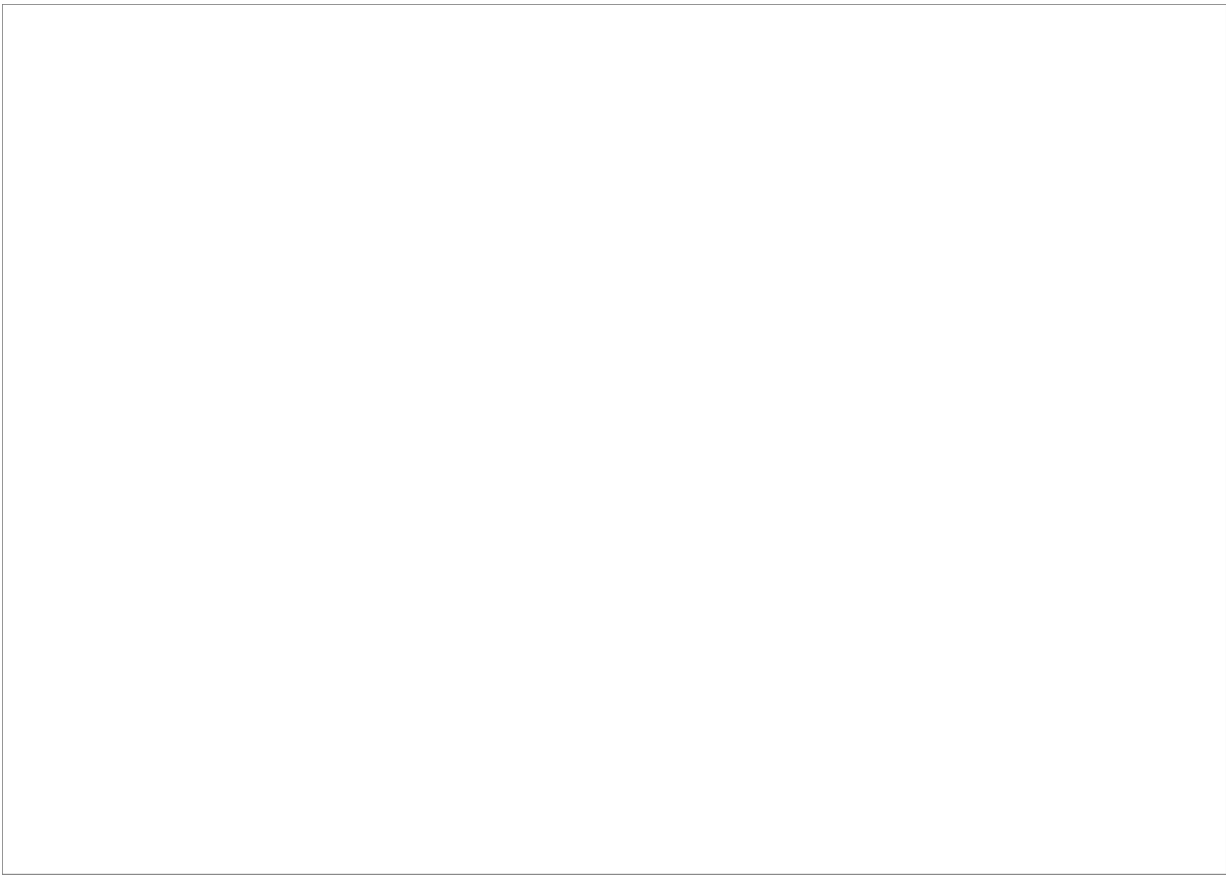
Fig. 2. Distribution of SiC particles in as-plated composite NiP–SiC coatings deposited from a bath with 80 g/l of 600 nm SiC particles: (a) as-plated, (b) after heat treatment at 420 °C for 1h.

Fig. 3. Polished cross-section of an as-plated composite NiP–SiC coating obtained from a bath with 80 g/l of 600 nm SiC particles.

The XRD pattern of as-plated NiP–SiC coatings consist mainly of a broad peak typical for amorphous material, and a sharp peak identified as silicon (Fig. 4). The as-plated NiP coatings also exhibit an amorphous peak. Low angle diffraction scans did not reveal any gradient in coating structure with depth. In line with previous investigations [14], [15] and [16], a substantial change in the structure of composite NiP–SiC and NiP coatings occurred after annealing at 420 °C. The matrix structure became a mixture of two phases, namely a crystalline SiC and Ni_3P phase (Fig. 5). A segregation of phosphorus in the grain boundaries and at triple junctions of NiP grains can occur with increasing temperature, leading to the formation of P-enriched zones. The precipitation of Ni_3P phase occurs when P-rich zones exceed a certain phosphorus limit, which has to be close to the eutectic concentration, namely 11 wt.% P [15]. Ni_3P precipitates are preferentially located at grain boundaries and triple junctions [17] and [18]. The process is controlled by diffusion, and the activation energy is similar to that of self-diffusion of pure nickel [19]. It is assumed that at 420 °C, nickel atoms migrate easily through P-rich zones and react with phosphorus to form Ni_3P

compounds. From the XRD investigation, it seems that the incorporation of SiC particles does not influence the structure of the as-deposited NiP matrix, which is in good agreement with literature [14].

Fig. 4. XRD patterns of as-plated composite NiP–SiC coatings deposited from a bath with 80 g/l of 600 nm SiC particles.

Fig. 5. XRD patterns of heat-treated composite NiP–SiC coatings deposited from a bath with 80 g/l of 600 nm SiC particles.

The variation of the coefficient of friction with wear testing time is shown in Fig. 6 and Fig. 7 for as-plated and annealed NiP composite coatings, respectively. Mean values from three sliding tests are shown for the composite NiP–SiC coatings and mean values from duplicated tests for NiP coatings deposited under identical conditions. The results appear quite reproducible. The coefficient of friction was found to be almost independent of the normal load used. All NiP composite coatings were tested for 15,000 cycles. After the running-in phase that lasted for about 4000 cycles, the coefficient of friction is approximately 0.7 (Fig. 6) for as-plated pure NiP and composite NiP–SiC coatings, and approximately 0.75 (Fig. 7) for such heat-treated coatings. The coefficient of friction exhibits after the running-in phase a rather wavy character on which sharp jumps in the coefficient of friction are superimposed especially in the case of composite NiP–SiC coatings.

Fig. 6. Coefficient of friction of as-plated pure NiP and composite NiP–SiC coatings during uni-directional sliding tests against corundum balls. Wear test parameters: normal load 2 N, 0.1 m/s, contact frequency 1 Hz, non-lubricated, ambient air of 50% RH and 23 °C.

Fig. 7. Coefficient of friction of heat-treated (1 h at 420 °C) pure NiP and composite NiP–SiC coatings during uni-directional sliding tests against corundum balls. Wear test parameters: normal load 2 N, 0.1 m/s, contact frequency 1 Hz, non-lubricated, ambient air of 50% RH and 23 °C.

In an attempt to clarify the wear behavior of composite NiP–SiC coatings, the Vickers hardness of unworn coatings was measured and plotted versus the hardness of unworn coatings (Fig. 8). Compared to as-plated pure NiP coatings, a slight increase in Vickers hardness was noticed for as-plated composite Ni–SiC coatings produced from plating baths containing 80 or 200 g/l SiC particles. The embedded submicron sized SiC particles do not increase largely the load bearing capacity in comparison to embedded micron-sized particles. However, the Vickers hardness

increases on heat treatment at 420 °C for 1 h due to the precipitation of Ni_3P-particles in the NiP matrix. That increase in hardness is even quite large for composite NiP–SiC coatings with a high content of submicron sized SiC particles. The wear loss after uni-directional sliding tests on as-plated NiP and composite NiP–SiC coatings is almost comparable. With increasing content of SiC particles in the as-plated composite NiP coatings, a small increase in wear loss is noticed possibly linked to the abrasion effect of the hard SiC particles when they are pulled out from the coatings during sliding tests. Interesting is the lowering of the wear volume loss that resulted from the heat treatment of pure NiP and composite NiP–SiC coatings. That decrease in wear volume loss seems to be mainly due to the formation of Ni_3P precipitates in the metal matrix of all these coatings. In the case of composite NiP–SiC coatings, the increased sensitivity for crack formation around the SiC particles in the NiP matrix seems to be at the origin of the slightly higher wear volume loss on composite NiP–SiC coatings in comparison to NiP coatings. During sliding, the pull out of SiC particles from the NiP matrix can thus easily contribute to an additional abrasive wear loss component. An optimisation of the electrolytic codeposition and heat treatment parameters would probably result in lower wear rates in composite NiP–SiC coatings compared to pure NiP coatings.

Fig. 8. Wear volume loss after uni-directional sliding tests (15,000 contacts, 2 N, 0.1 m/s, 1 Hz, ambient air 50% RH and 23 °C) versus Vickers hardness for as-plated and heat-treated pure NiP and composite NiP–SiC coatings.
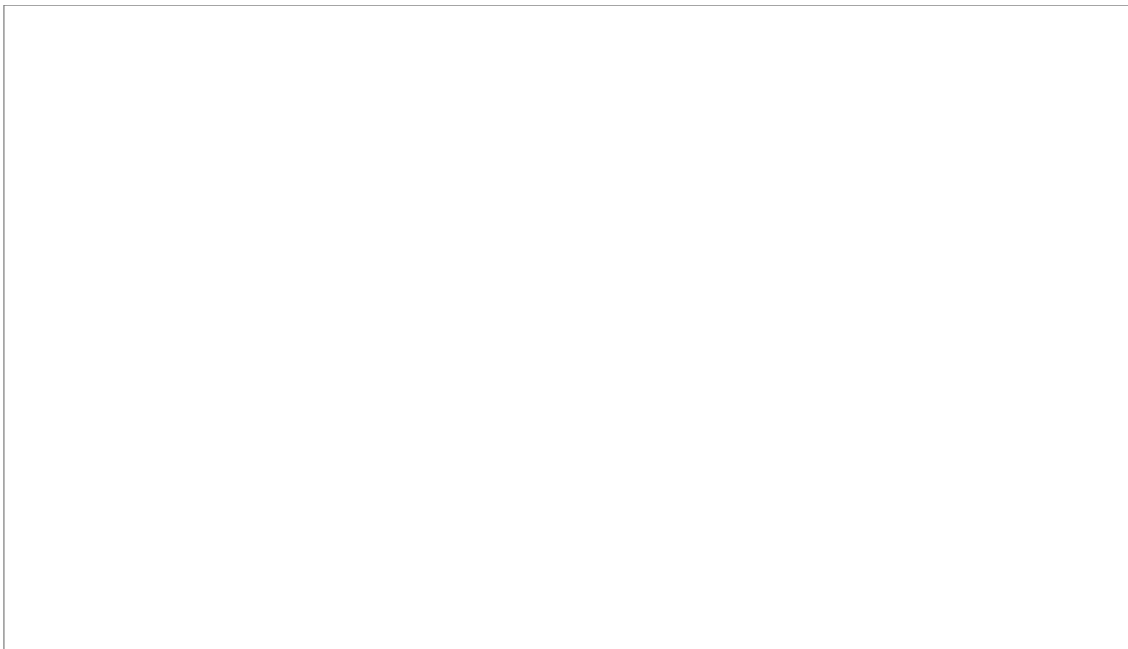
A SEM picture of a wear track on as-plated NiP–SiC coating is shown in Fig. 9. Some parts of this wear scar have a black appearance. Some scratches and cracks parallel to the direction of motion are also visible. Such scratches are typical for abrasive wear. The morphology of this wear track area is quite smooth, indicating that some polishing took place probably by fine pull out SiC particles. The appearance of all wear tracks on as-plated and heat-treated composite NiP–SiC coatings was similar and not dependent on the content of SiC particles in the composite coatings. Details of the black zones in the wear tracks on as-plated composite NiP–SiC coatings are shown in Fig. 10 and Fig. 11. In these black zones, a lot of small cracks perpendicular to the sliding direction are visible as well as some cracks in the sliding direction (Fig. 10). A further zoom-in reveals that in these black zones in the wear tracks, the pull out of SiC particles took place and that a lot of fine cracks are visible originating frequently from places where originally SiC particles were embedded (Fig. 11). This observation was done on all heat-treated composite NiP–SiC coatings.

Fig. 9. Microstructure of the wear tracks on as-plated composite NiP–SiC coatings (600 nm 80 g/l). Uni-directional wear test parameters: corundum ball as counter body, 2 N; 0.1 m/s, 1 Hz, 15,000 contacts, ambient air 50%RH and 23 °C.
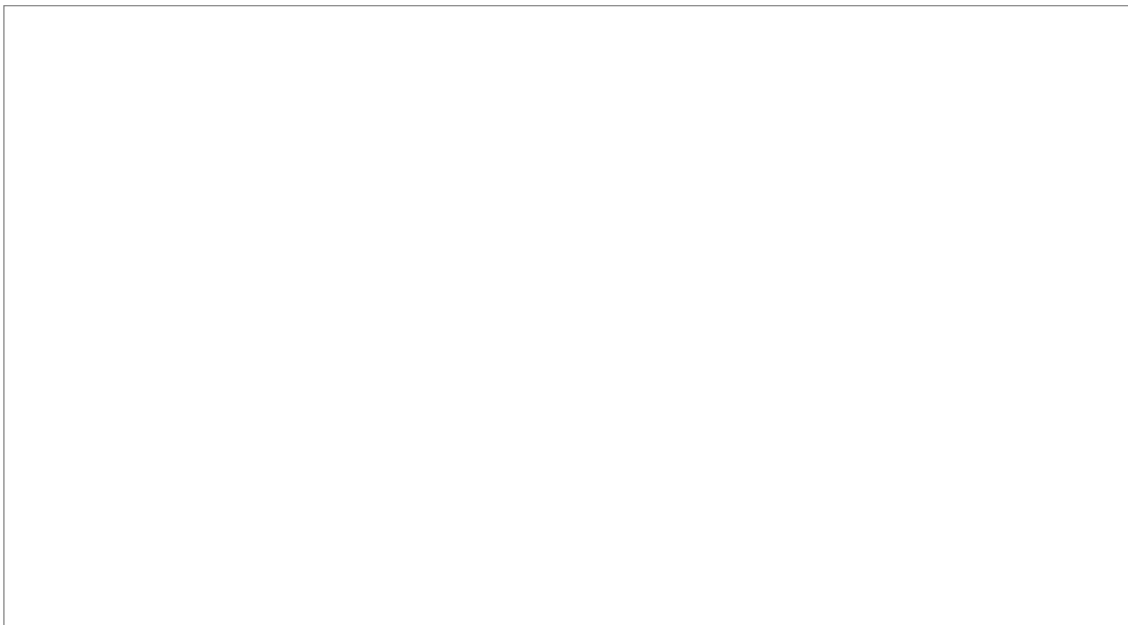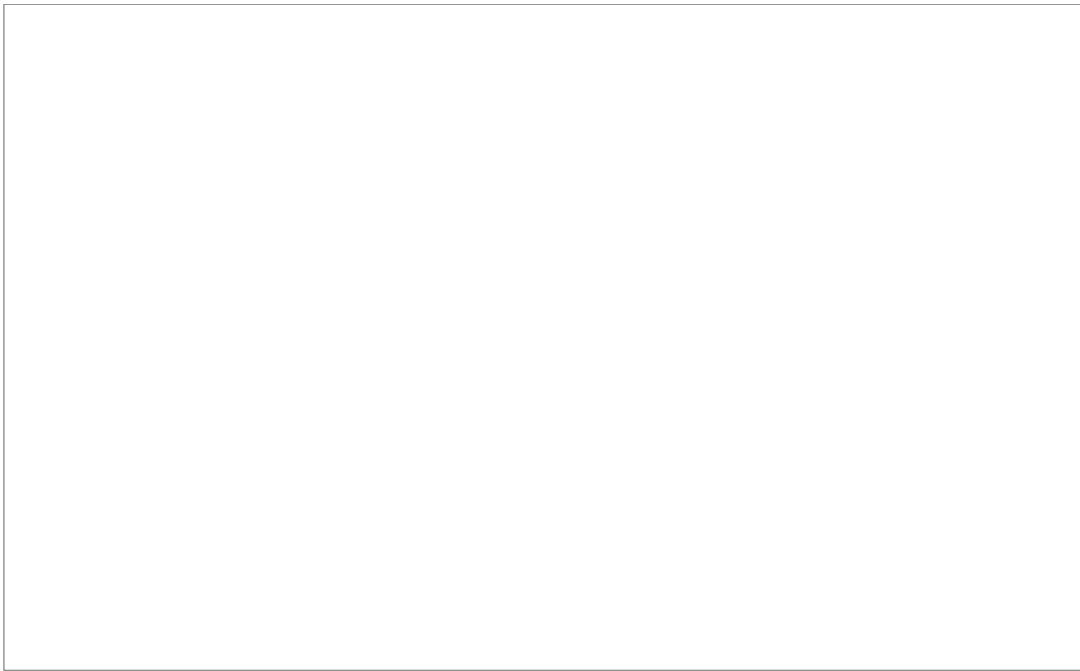
Fig. 10. Details of black area in Fig. 8.

Fig. 11. Details of black area in Fig. 9.

The formation of black bands in the wear tracks was also noticed on as-plated and heat-treated pure NiP coatings but to a larger extent than on composite NiP–SiC coatings. These black bands are parallel to the direction of motion and the sequence in the formation of such black bands on heat-treated pure NiP coatings can be derived from Fig. 12a to c. These SEM micrographs were taken after uni-directional sliding tests performed at increasing number of rotations. After the first 100 sliding contacts, some scratches parallel to the direction of motion are observed in the wear track. This observation is in agreement with the findings of Chen et al. [7] who reported scratches after 400 cycles on NiP coatings subjected to sliding wear tests against SiC paper. On increasing the number of sliding contacts in our study from 100 to 1000, the wear behavior evolves from abrasive wear to oxidational wear. Indeed, chemical analyses by EDX did not reveal any substantial amount of oxygen in the wear track area after 100 contacts, while after 1000 and 15,000 sliding contacts, the presence of oxygen was clearly detected in the black areas in the wear tracks. The amount of oxygen increases with increasing number of sliding contacts (see Table 1). The formation of the oxide film was found to evolve identically in both as-plated and heat-treated samples with the number of sliding contacts. The compositional analysis of the wear track of all coatings investigated is given in Table 1. The oxygen content in the wear tracks of all as-plated coatings appears similar. For annealed coatings, the chemical oxygen content in the wear tracks on NiP coatings is

approximately 10 times higher than in the wear track on composite NiP–SiC coatings. The chemical content of oxygen in the wear track area on NiP coatings is also dependent on the number of sliding cycles. A significant difference in the intensity level of oxygen between the center of wear tracks and heat-treated NiP–SiC coatings, was not detected.

Fig. 12. Evolution of the formation of oxide films on heat-treated NiP coatings after uni-directional sliding tests performed at 2 N, 0.1 m/s, in ambient air 50% RH and 23 °C for: (a) 100 contacts, (b) 1000 contacts, (c) 15,000 contacts.
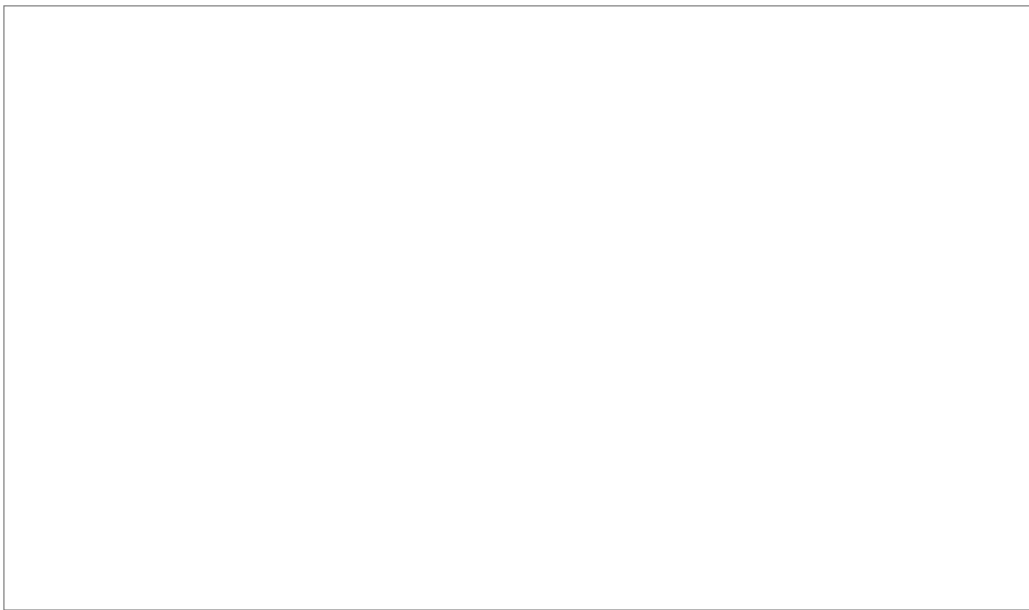
An interesting finding resulted from an investigation of the wear track morphology on as-plated pure NiP coatings after ultrasonic cleaning in ethanol for 15 min (Fig. 13). Ultrasonic cleaning did remove the oxide film formed after a low number of sliding contacts (compare Fig. 12 and Fig. 13). Notice the relatively deep grooves visible after ultrasonic cleaning (Fig. 13b) indicating that both

oxidational and abrasive wear are active in uni-drectional sliding tests on NiP coatings as well. However, ultrasonic cleaning did not remove the oxide films formed in wear tracks after an extended number of sliding contacts (compare Fig. 12 and Fig. 13). This indicate that the oxidation of the NiP matrix material result in a good adhering surface films that thus can protect the underlying coating material from further wear.

Fig. 13. Evolution of the formation of oxide films on as-plated NiP coatings after uni-directional sliding tests performed at 2 N, 0.1 m/s, in ambient air 50% RH and 23 °C for: (a) 100 contacts, (b) 1000 contacts, (c) 15,000 contacts. Micrographs taken after ultrasonic cleaning for 15 min in ethanol.
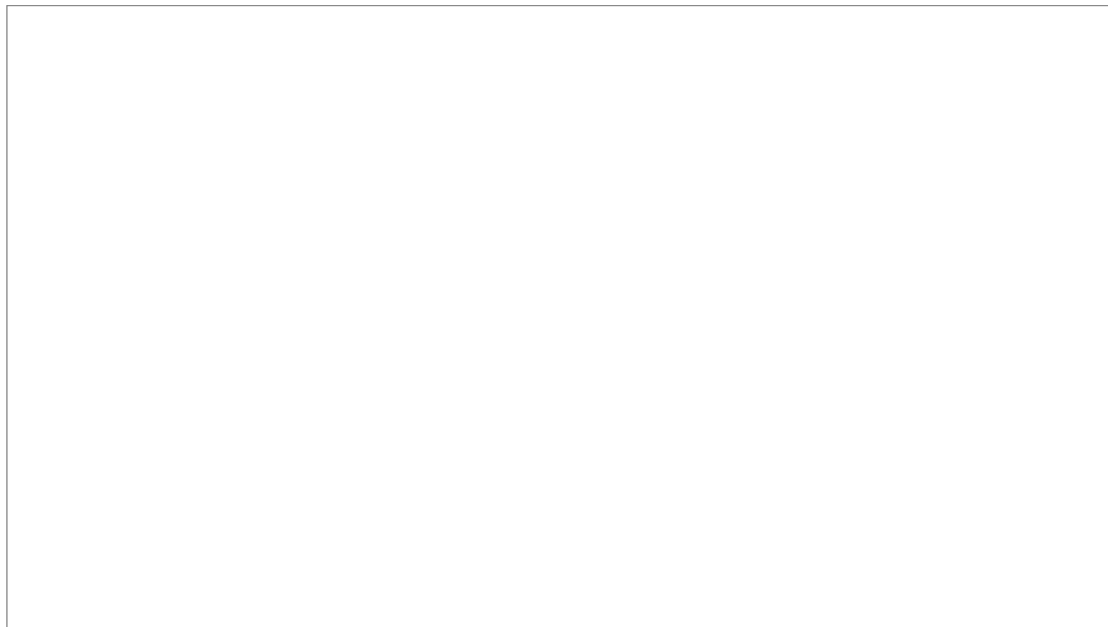
The wear of these pure NiP and composite NiP–SiC coatings seems thus to result from a competition between abrasive wear and oxidational wear, the first one leading to a progressive material loss, the second one leading to a temporary protection of the underlying material. The wear mechanism is typically an abrasive one in the case of as-plated and heat-treated composite NiP–SiC coatings. On the contrary, in as-plated and heat-treated NiP coatings, the presence of an oxide film indicates an oxidational wear. It seems that the presence of SiC particles in NiP coatings not only

increases the hardness but also reduces the extent of oxidation since oxide layers were scarcely noticed inside the wear track on these composite coatings. In such cases, only abrasive scars were observed. This competition of oxidational and abrasive wear could also be the explanation for the different evolution of the coefficient of friction for pure NiP and composite NiP–SiC coatings with increasing numbers of contacts noticed in Fig. 6 and Fig. 7. In the case of composite NiP–SiC coatings, the sharp jumps in the coefficient of friction could be due to a periodic pull out of SiC particles from the wear track area generating an intense abrasive wear. While in the case of NiP coatings, the progressive growth and subsequent breaking up of a surface oxide layer could explain the more smooth and wavy character of the coefficient of friction with test duration observed on such coatings.

The wear debris located at the ends of the sliding wear scars can be easily removed by rinsing with distilled water. The microstructure of such debris is shown in Fig. 14. EDAX analyses revealed the presence of O and Al in these wear debris in addition to Ni and P. The aluminum is due to debris originating from the corundum counter body and the amount of oxygen and aluminum was found to be identical for all coatings investigated (see Table 1). The amount of oxygen is relatively higher in the debris ejected from the sliding contact area.

Fig. 14. Microstructure of debris formed during uni-directional sliding test performed at 2 N, 0.1 m/s, 1 Hz in ambient air 50% RH and 23 °C for 15,000 cycles on as-plated composite NiP–SiC (600 nm, 80 g/l).

Finally, a SEM investigation of the corundum counter body revealed that a layer of wear debris adheres on the corundum surface around the contact zone with numerous cracks and fragmentation at the edges (Fig. 15). Abrasive SiC particles adhering on the surface of the counter body are clearly visible in that layer (Fig. 16). The chemical composition of that layer confirmed the transfer of materials from the coatings. Since the wear on the counter body materials is very limited, it was not possible to estimate any wear volume loss on it by profilometry.

Fig. 15. SEM micrograph of corundum counter body showing a transfer layer adhering at the periphery of the contact zone. Counter body: as-plated composite NiP–SiC coating (600 nm, 80 g/l).

Uni-directional sliding test parameters: 2 N, 0.1 m/s, 1 Hz, 15,000 cycles, ambient air 50% RH and 23 °C. Black arrow indicates sliding direction of counter body.
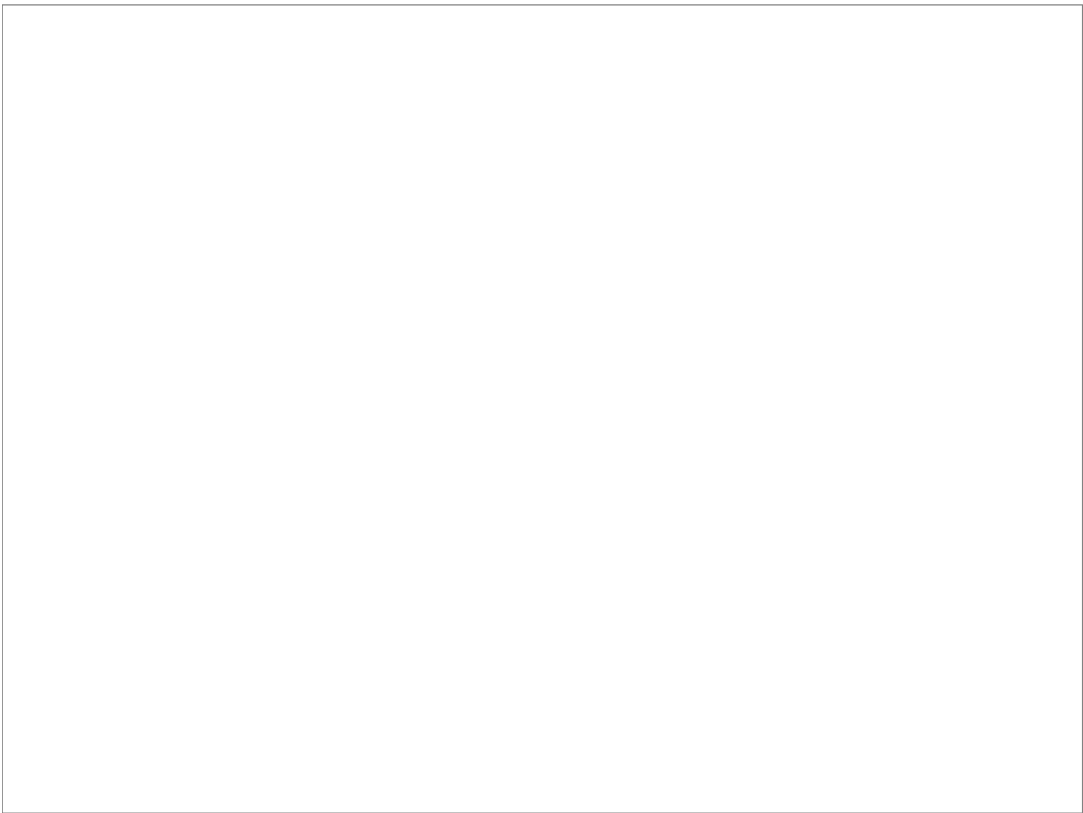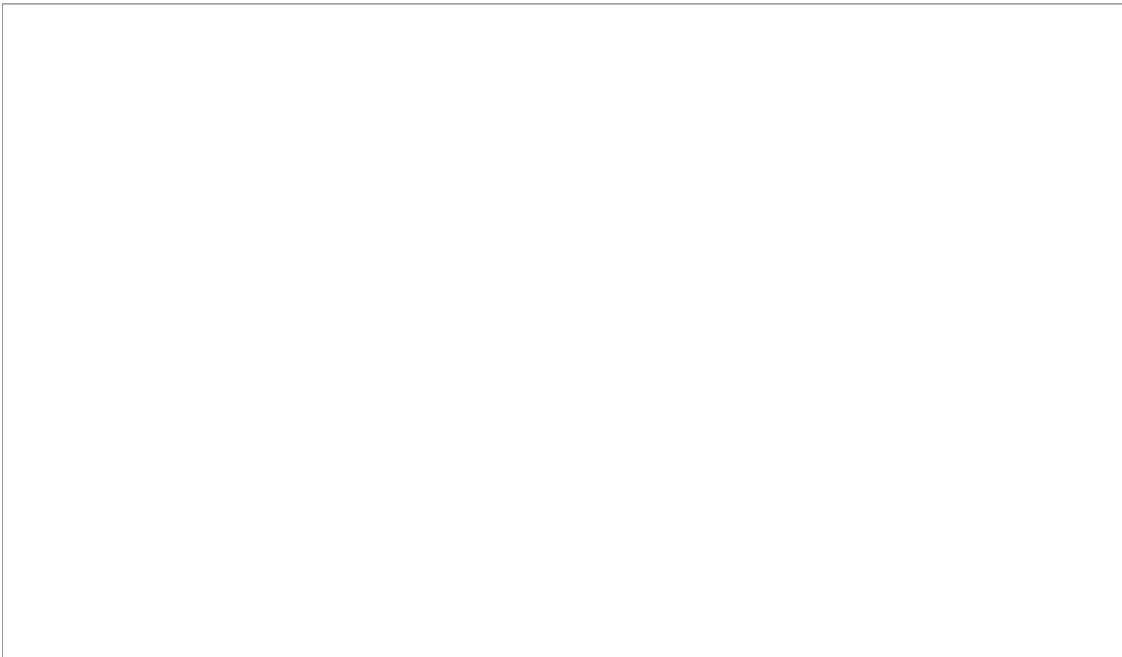
Fig. 16. SEM micrograph of transfer layer on corundum counter body after uni-directional sliding test against as-plated composite NiP–SiC coating (600 nm, 80 g/l) performed at 2 N, 0.1 m/s, 1 Hz, in ambient air 50% RH and 23 °C. Details of central area in Fig. 14.

4. Conclusions

The friction and wear behavior of NiP and composite NiP–SiC coatings were shown to depend on the presence of reinforcing Ni_3P and SiC particles in the coatings. Submicron SiC particles are embedded in the metal matrix during the electrodeposition of the coatings and thus the electroplating parameters determine their content. On the contrary, the Ni_3P particles result from a precipitation reaction during a subsequent heat treatment of the coatings and their amount depends on the phosphorus incorporation during electroplating but also on the heat treatment parameters used.

The mean friction values of NiP and composite NiP–SiC coatings in uni-directional sliding tests are almost not affected by the presence of SiC and Ni_3P particles. However, typical variations in the coefficient of friction during such uni-directional sliding tests reveal that different wear processes

are taking place. In the case of composite NiP–SiC coatings, the oxidation of the NiP matrix is apparently hindered by the SiC particles in comparison to pure NiP coatings but abrasive wear is promoted. That increased abrasion wear can result from hard SiC particles embedded in the metal matrix or on pull out, followed by an entrapment in the contact area or a transfer of these particles to the counter body. This competition between oxidational and abrasive wear was noticed in the as-plated conditions as well as in heat-treated conditions for composite NiP–SiC coatings. To some extent such a competition between oxidational and abrasive wear was also noticed on pure as-plated and heat-treated NiP. A major difference was noticed, namely that the oxidation film formed in the wear track area on NiP under uni-directional sliding adheres strongly to the coating protecting it from a high wear rate.

The best uni-directional sliding wear resistance against corundum balls was obtained in this study with heat-treated pure NiP coatings. The electrodeposition and heat treatment of composite NiP–SiC coatings need further optimization in order to limit the crack sensitivity that results in a pull out of embedded SiC particles contributing to an enlarged abrasive wear.

Acknowledgements

References

I. Garcia, D. Drees and J.-P. Celis, *Wear* 249 (2001), p. 452.

S. Wang, R. Rofagha, P.R. Roberge and U. Erb, *Electrochem. Soc., Proc.* 95 (1995) (8), p. 244.

P. Pouderoux, I. Chassaing, J.P. Bonino and A. Rousset, *Surf. Coat. Technol.* 45 (1991), p. 161.

W. Paatsch, *Metalloberflache* 40 (1986), p. 387.

I. Garcia, J. Fransaer and J.-P. Celis, *Surf. Coat. Technol.* 148 (2001), p. 171.

B. Gillot, K. El Amri, P. Pouderoux and A. Rousset, *J. Alloys Compd.* 189 (1992), p. 151.

C.K. Chen, H.M. Feng, H.C. Lin and M.H. Hon, *Thin Solid Films* 416 (2002), p. 31.

I. Apachitei, E.D. Tichelaar, J. Duszczyk and L. Katgerman, *Surf. Coat. Technol.* 149 (2002), p. 263.

F. Hubbel, *Trans. Inst. Met. Finish.* 56 (1978), p. 65.

N. Feldstein In: G.O. Mallory and J.B. Hajdu, Editors, *Electroless Platting: Fundamentals and Applications*, American Electroplaters and Surface Finishers Society, Orlando, FL (1990), p. 269.

Y.S. Huang, X.T. Zeng, I. Annergren and F.M. Liu, *Surf. Coat. Technol.* 167 (2003), p. 207.

R. Taheri, I.N.A. Oquocha and S. Yannacopoulos, *Wear* 249 (2001), p. 389.

O. Berkh, S. Eskin and J. Zahavi, *Metal Finish.* 94 (1996), p. 35.

I. Apachitei and J. Duszczyk, *Surf. Coat. Technol.* 132 (2000), p. 89.

T. Hentschel, D. Isheim, R. Kirchheim, F. Muller and H. Kreye, *Acta Mater.* 48 (2000), p. 933.

B. Farber, E. Cadel, A. Menand, G. Schimitz and R. Kirchheim, *Acta Mater.* 48 (2000), p. 789.

K. Boylan, D. Ostrander, U. Erb, G. Palumbo and K.T. Aust, *Scr. Metall. Mater.* 25 (1991), p. 2711.

S.C. Mehta, D.A. Smith and U. Erb, *Mater. Sci. Eng., A* 204 (1995), p. 227.

A.K. Jena and M.C. Chaturvedi, *Phase Transformation in Materials*, Prentice Hall, Englewood Cliffs (1992), p. 103.

Corresponding author. Katholieke Universiteit Leuven, Departement Metaalkunde en Toegepaste Materiaalkunde, Kasteelpark Arenberg 44, B-3001 Leuven, Belgium. Tel.: +32 7 3472 39 18 74; fax: +32 7 3472 25 37 59.

Original text : Elsevier.com